Biochemical and Biophysical Research Communications 460 (2015) 504–510

Contents lists available at ScienceDirect

Biochemical and Biophysical Research Communications

journal homepage: www.elsevier.com/locate/ybbrc

Pyruvate metabolism: A therapeutic opportunity in radiation-induced skin injury

Hyun Yoo [a], Jeong Wook Kang [a], Dong Won Lee [b], Sang Ho Oh [c], Yun-Sil Lee [d], Eun-Jung Lee [a], Jaeho Cho [a, *]

[a] Department of Radiation Oncology, Yonsei University College of Medicine, 50 Yonsei-ro, Seodaemun-gu, Seoul 120-752, South Korea
[b] Department of Plastic Surgery, Yonsei University College of Medicine, 50 Yonsei-ro, Seodaemun-gu, Seoul 120-752, South Korea
[c] Department of Dermatology, Yonsei University College of Medicine, 50 Yonsei-ro, Seodaemun-gu, Seoul 120-752, South Korea
[d] College of Pharmacy & Division of Life and Pharmaceutical Sciences, Ewah Womans University, Seoul 120-750, South Korea

ARTICLE INFO

Article history:
Received 9 March 2015
Available online 19 March 2015

Keywords:
Radiation
Skin injury
Pyruvate dehydrogenase kinase

ABSTRACT

Ionizing radiation is used to treat a range of cancers. Despite recent technological progress, radiation therapy can damage the skin at the administration site. The specific molecular mechanisms involved in this effect have not been fully characterized. In this study, the effects of pyruvate, on radiation-induced skin injury were investigated, including the role of the pyruvate dehydrogenase kinase 2 (PDK2) signaling pathway. Next generation sequencing (NGS) identified a wide range of gene expression differences between the control and irradiated mice, including reduced expression of PDK2. This was confirmed using Q-PCR. Cell culture studies demonstrated that PDK2 overexpression and a high cellular pyruvate concentration inhibited radiation-induced cytokine expression. Immunohistochemical studies demonstrated radiation-induced skin thickening and gene expression changes. Oral pyruvate treatment markedly downregulated radiation-induced changes in skin thickness and inflammatory cytokine expression. These findings indicated that regulation of the pyruvate metabolic pathway could provide an effective approach to the control of radiation-induced skin damage.

© 2015 Elsevier Inc. All rights reserved.

1. Introduction

Radiation therapy is widely used to treat a range of cancers, but it can result in varying degrees of damage to normal skin at the site of administration [1,2]. Radiation-induced skin injury involves morphological and functional changes that occur in acute and late skin injury. Acute skin damage occurs hours to weeks after exposure and it is characterized by early/faint transient erythema, dry/moist desquamation, and ulceration. Late skin damage typically occurs months to years after exposure and it is characterized by fibrosis, dermal necrosis/atrophy, loss of hair follicles, telangiectasia, and delayed ulceration [1,2]. Some treatments such as pentoxifylline and vitamin E were reported to reduce radiation-induced skin fibrosis [3,4]. However, there are no other currently available therapies for radiation-induced skin injury. Therefore, understanding the mechanisms involved in radiation-induced skin damage could contribute to the development of novel therapeutics.

There are many differences in glucose metabolism in normal and cancerous tissues. Normal tissues metabolize glucose to produce energy via oxidative phosphorylation whereas in cancer cells, 90% of total glucose is converted to lactose; this is known as the Warburg effect [5]. Glycolysis involves many enzymes and pyruvate dehydrogenase kinase (PDK) and the pyruvate dehydrogenase complex (PDC) play important roles in glucose metabolism. The PDC-catalyzed conversion of pyruvate, the final product of glycolysis, into acetyl-CoA is one of the entry points into the citric acid cycle. PDC is a multi-subunit complex that is activated by dephosphorylation by pyruvate dehydrogenase phosphatases (PDPs) and inactivated via PDK-catalyzed phosphorylation [6,7]. There are four known PDK isoenzymes in mammals: PDK1 is mainly expressed in the heart, PDK2 in most tissues, PDK3 in testis, and PDK4 shows the highest expression levels in heart and skeletal muscle [8].

Cellular pyruvate concentration is believed to play a role in the pathogenesis of skin disorders, by increasing the expression of cell proliferation factors. However, the specific molecular mechanism involved in pyruvate's influence on skin hyperplasia remains to be

* Corresponding author. Fax: +82 2 312 9033.
E-mail address: jjhmd@yuhs.ac (J. Cho).

http://dx.doi.org/10.1016/j.bbrc.2015.03.060
0006-291X/© 2015 Elsevier Inc. All rights reserved.

elucidated. Therefore, the present study investigated the effects of pyruvate on radiation-induced skin injury. We found that oral administration of pyruvate inhibited radiation-induced changes in mouse skin thickness and downregulated the expression of several inflammatory cytokine genes.

2. Methods and materials

2.1. Materials

Normal and sodium pyruvate-free culture media both contained 10% fetal bovine serum (Gibco/Hyclone BRL, Rockville, MD, USA). Normal DMEM (SH30243.01) was high-glucose DMEM containing L-glutamine (4 mM) and sodium pyruvate (110 mg/L). Sodium pyruvate-free DMEM (SH30022.01) was high-glucose DMEM with L-glutamine (4 mM) and no sodium pyruvate. Antibodies to PDK2 and the Pyruvate Assay Kit were purchased from ABcam (Beverly, MA, USA). The β-actin antibody was purchased from Santa Cruz Biotechnology (Santa Cruz, CA, USA). Pyruvate was purchased from Sigma (Woburn, MA, USA). A PDK2 plasmid (PDK2-pCMV-SPORT6 clone) was provided by the Korea Human Gene Bank, Medical Genomics Research Center, Korea Research Institute of Bioscience & Biotechnology, Korea.

2.2. Cell culture

The NIH3T3 immortalized mouse fibroblast cells were grown in Dulbecco's modified Eagle's medium supplemented with 10% fetal bovine serum, 100 units/mL penicillin, and 100 mg/mL streptomycin at 37 °C in a humidified 5% (v/v) CO_2 atmosphere. The cells were seeded at 1.0×10^6 cells/100 mm plate. After 24 h, the cells were washed with serum-free medium and maintained in serum-free medium prior to the experiments.

2.3. Transfection

Transient transfections were performed by using Efectene according to the manufacturer's protocol (Qiagen; Santa Clara, CA, USA). In brief, 5.0×10^5 cells were plated in a 60 mm dish 1 day prior to the transfection and grown to approximately 70% confluence. They were then transfected with plasmid DNA at a concentration of 1 mg/plate. The transfections were allowed to proceed for 24 h, and the transfected cells were harvested.

2.4. Quantitative real-time polymerase chain reaction (Q-PCR)

Total RNA was isolated from the cells using the TRIzol reagent from Invitrogen (Carlsbad, CA, USA) according to the manufacturer's instructions. cDNA was synthesized using the Quantifect Reverse Transcription Kit (Qiagen, Hilden, Germany). For Q-PCR, SYBR Premix Ex Tag (Takara, Otsu, Japan) was mixed with each primer, RNase-free H_2O, and cDNA to achieve a final reaction volume of 20 μL. The following parameters were used for Q-PCR: 95 °C for 10 min, followed by 50 cycles of 95 °C for 20 s, 55 °C for 30 s, and 72 °C for 20 s. All experiments were conducted in triplicate and data were normalized to glyceraldehyde-3-phosphate dehydrogenase expression.

2.5. Pyruvate assay

NIH3T3 cells were maintained for 24 h in pyruvate-free and normal media prior to the transfection or irradiation. Cells were transfected or not with PDK2 plasmid before irradiation. After irradiation, the cells were cultured without pyruvate and then harvested. Pyruvate concentration was quantified using a Pyruvate assay Kit (ab65342) according to the manufacturer's protocol (abcam, UK).

2.6. RNA-seq

To compare the gene expression profiles of irradiated and non-irradiated skin, we performed RNA-seq analysis using Illumina-based next generation sequencing (NGS). Total RNA was isolated from mouse flank skin using TRIzol, quantitated using a Nanodrop spectrophotometer and quality-assessed using the RNA 6000 Nano assay kit (Agilent Technologies, CA, USA) and a Bioanalyzer 2100 (Agilent). mRNA was isolated from total RNA using oligo-dT magnetic beads and NGS sequencing libraries were generated using the Illumina TruSeq library kit, according to the manufacturer's protocol. The constructed libraries were then paired-end sequenced (2X101bp) on the Illumina HiSeq™ 2000 system. Sequencing artifacts (such as the universal adapters) were removed using Trimmomatic [9] with the parameter options 'ILLUMINACLIP:2:30:10 MINLEN:75' before read alignment. The *Mus musculus* genome (GRCm38) sequence and gene information were downloaded from Ensembl (release 73) and quality-filtered reads were aligned using TopHat [10]. Aligned reads were sorted using SAMtools [11] and HTseq [12] was used to calculate the read count for each gene. To identify the effect of irradiation on gene expression, we used the R package DESeq [13], which is based on a negative binomial model. DEGs (p value < 0.01, Bonferroni corrected) were categorized by gene ontology (GO) using the DAVID [14] web tool and a modified Fisher's exact test was used to measure enrichment of GO terms.

2.7. Radiation delivery and dosimetry

Radiation was delivered with an X-RAD 320 (Precision, North Branford, CT, USA), equipped with fixed and adjustable collimation fixtures. The collimators produced a beam with a 1 cm × 1 cm coverage area. The percentage depth doses (PDDs) were measured after absolute dosimetric measurements with GAFCHROMIC EBT3 film and acrylic and water-equivalent RW3 slab phantoms (PTW, RW3). The aluminum-filtered X-ray beam dose rate was 8.3 cGy/s, measured at 320 kV and 12.5 mA using a cylindrical ionization Farmer-type chamber (PTW 0.6 cm^2, waterproof) within an RW3 phantom at a source-to-surface distance of 2 cm. The output was calibrated as recommended by the American Association of Physicists in Medicine, TG-61 report [15].

Radiation dosimetry for cultured cells was carried out using a cell culture dish, water, an RW3 phantom slab, and GAFCHROMIC EBT3 film. The cell culture dishes were filled with 10 mL water. EBT3 film was placed in the bottom of each dish for radiation measurement. Radiation delivered to the EBT3 films was converted to dose value using a PDD calibration curve (optical density-pixel value plotted against radiation dose [cGy]). In this experiment, cells were administered 10 Gy in one fraction.

2.8. In vivo irradiation and oral administration of pyruvate

All studies involving mice were approved by the Yonsei University Medical School Animal Care and Use Committee. Five male adult (6-week-old) C57BL/6 mice were housed per cage and allowed to acclimate for one week after arrival. A 1 cm × 1 cm collimator was used to administer a single dose of 50 Gy to the dorsal skin of 6 mice [16]. During irradiation, the mice were anesthetized with an intraperitoneal injection of 30 mg/kg Zoletil (tiletamine and zolazepam) and 10 mg/kg of Rompun (xylazine). Pyruvate was dissolved in distilled water and mice were given an oral dose (500 mg/kg) of pyruvate or vehicle control every two days after irradiation [17,18]. Six weeks after these procedures, the mice

were sacrificed. The experiment was repeated twice, with nine mice per group on each occasion.

2.9. Statistical analysis

The difference between the two study group means was evaluated using Student's t-test. Differences between multiple group means were evaluated using a one-way analysis of variance (ANOVA), followed by Dunnett's multiple comparison test. The threshold for statistical significance was $p < 0.05$ for both tests.

3. Results

3.1. Radiation-induced skin thickening

The effect of radiation on skin thickness was examined in mouse dorsal skin [16]. Changes became obvious at 4 weeks and continued to progress over the 6-week study period. Progressive morphological changes characteristic of radiation injury were observed, including epidermal hyperplasia, interface dermatitis, loss of hair follicles, hyperkeratosis, and dermal fibrosis. Moreover, thickening of the skin, with substantial and progressive collagen deposition over time, was observed after Masson's Trichrome staining (Fig. 1).

3.2. The effect of irradiation on PDK2 gene expression

RNA expression profiles in normal and irradiated mouse skin tissue were examined using RNA-seq. We identified 682 differentially expressed genes and classified these using DESeq; 334 were upregulated and 348 were downregulated. GO term enrichment analysis revealed preferential radiation-related decreases in the expression of genes involved in a range of biological process including cell proliferation, tube development, oxidation/reduction, and several metabolic processes. S. Table 1 shows the sequencing results by GO pathway (12 glucose metabolism-related genes) for downregulated genes, $p < 0.05$ (Fig. 2A and B). PDK2 gene expression was reduced following exposure to radiation. To investigate this further, Q-PCR analysis was performed of irradiated NIH3T3 cells and mouse skin. These data (Fig. 2C) also showed that exposure to radiation drastically decreased the PDK2 mRNA level. As shown in Fig. 2D, histological analysis indicated that PDK2 protein expression was decreased by irradiation.

3.3. PDK2 inhibited irradiation-induced cytokine gene expression

Next, we investigated PDK2-induced expression of cytokines and chemokines. NIH3T3 cells were transfected with a PDK2 plasmid prior to irradiation. We observed that radiation-mediated cytokine induction was downregulated in cells transfected with PDK2 and cytokine levels subsequently returned to the control levels (Fig. 3A and B).

3.4. Induction of cytokine gene expression by pyruvate deficiency in NIH3T3 cells

We previous examined PDK2 expression by Q-PCR analysis and hypothesized that irradiation might influence cellular pyruvate concentration. The present study therefore employed Pyruvate assay kit to investigate the effects of irradiation on pyruvate levels in NIH3T3 cells. As shown in Fig. 3C, extracellular pyruvate levels were decreased by irradiation. NIH3T3 cells were transfected with the respective rescue constructs, followed by transfection with PDK2. These results demonstrated that the radiation-induced reduction in pyruvate expression was mediated through a PDK2 pathway. To determine whether the same molecular mechanism was involved in irradiation-induced cytokine expression and PDK2 over-expression, the effects of pyruvate on cytokine expression were examined. Irradiation-induced cytokine gene expression was assessed in NIH3T3 cells after 24-h treatment with normal, or pyruvate-free, media. The data presented in Fig. 3D indicated that irradiation of cells incubated with pyruvate-free medium produced a much greater increase in cytokine mRNA levels, as compared with cells incubated with normal medium. This finding was consistent with our observation that a high concentration of pyruvate inhibited radiation-induced cytokine gene expression.

3.5. Pyruvate inhibited radiation-induced skin injury

Histological examination identified ulceration, areas of dermal necrosis, and areas of dermal thickening, fibrosis, alopecia, edema,

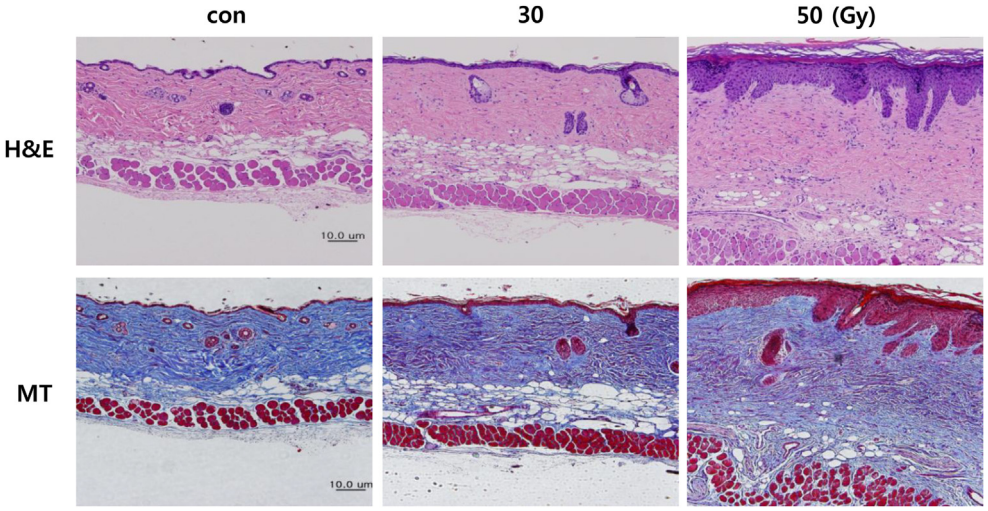

Fig. 1. Radiation-induced increase in skin thickness. Representative images of sections of 30, 50-Gy irradiated skin sampled at 6 weeks and stained with hematoxylin and eosin (H&E) or Masson's Trichrome (MT; connective tissue, blue; nuclei, dark red/purple; cytoplasm, red/pink). Irradiated sections demonstrated marked thickening of both the epidermis and dermis (×100). (For interpretation of the references to color in this figure legend, the reader is referred to the web version of this article.)

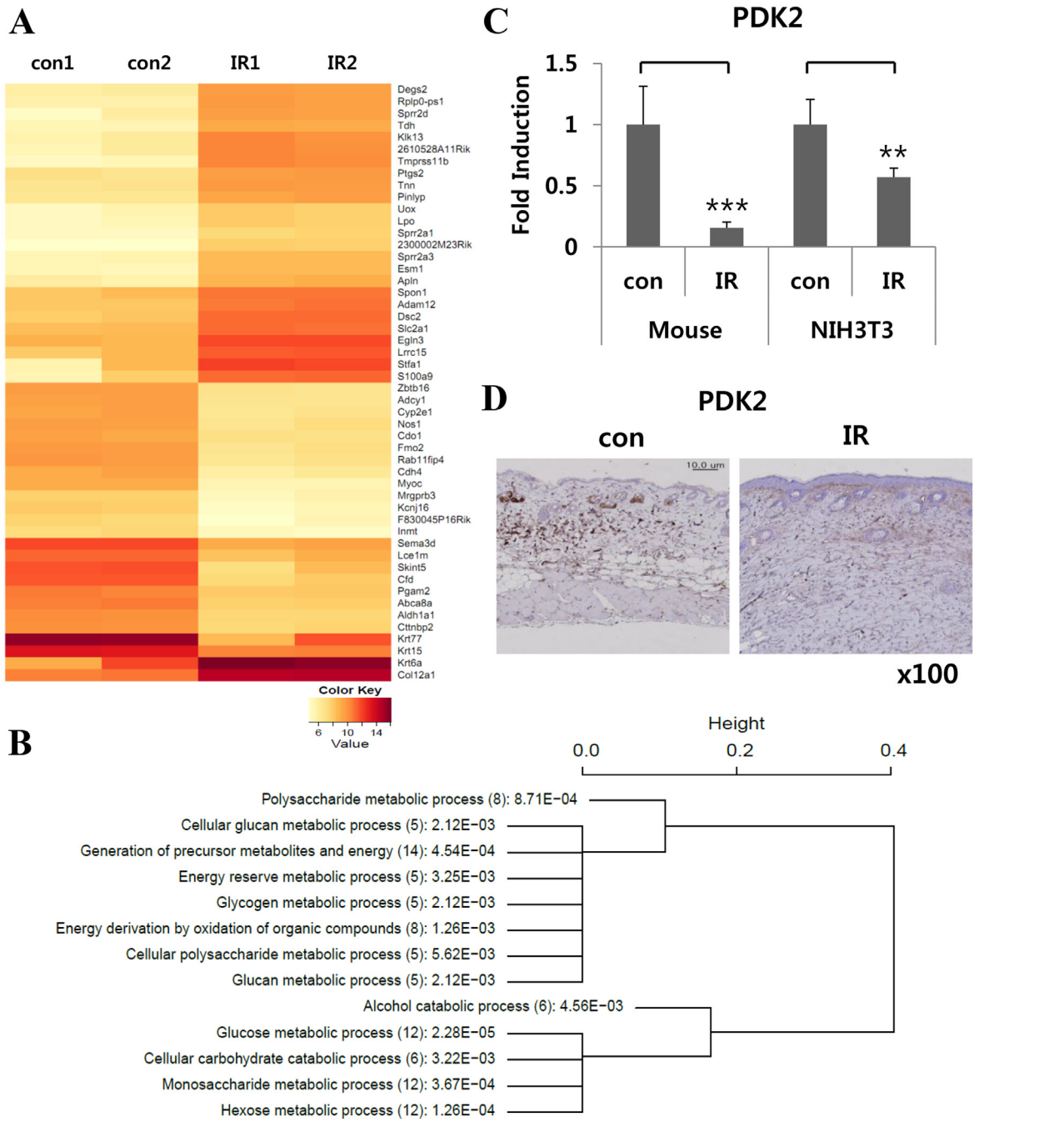

Fig. 2. The effect of irradiation on pyruvate dehydrogenase kinase 2 (PDK2) gene expressions. A) RNA-seq analysis heatmap of differential gene expression between the control and irradiated mouse skin. The expression level of each gene in the heatmap is scaled and represented as z-scores. B) Gene enrichment and gene ontology pathway (biological process) analysis of RNA-seq expression profiles, showing an enrichment of glucose metabolism-related genes. C) Quantitative real-time PCR analysis showed that irradiation decreased PDK2 gene expression in mouse skin and NIH3T3 cells, as indicated. Error bars show standard deviation; $^{**}p < 0.01$; $^{***}p < 0.001$. D) Immunohistochemical staining was performed on the mouse skin sections using an anti-PDK2 antibody (×100).

and cytokine production in mouse dorsal skin 6 weeks after radiation exposure [1,2]. These effects resembled the phenotypic characteristics of human radiation-induced skin injury. In this study, we investigated whether pyruvate attenuated the increase in skin thickness and collagen synthesis produced by radiation. As shown in Fig. 4B, oral pyruvate administration decreased epithelial thickening, hyperkeratosis, and dermal collagen accumulation. Pyruvate also significantly inhibited radiation-induced cytokine gene expression, determined by Q-PCR (Fig. 4C).

4. Discussion

The RNA-seq data revealed that genes related to glucose metabolism were significantly altered by skin irradiation and were worthy of further investigation; of these, PDK2 showed the most significant alteration. A number of studies have demonstrated glucose metabolism pathways in skin diseases [19–21] and the high efficiency of radio-sensitization [22,23]. Therefore, PDK2 is believed to play a role in the pathogenesis of skin diseases.

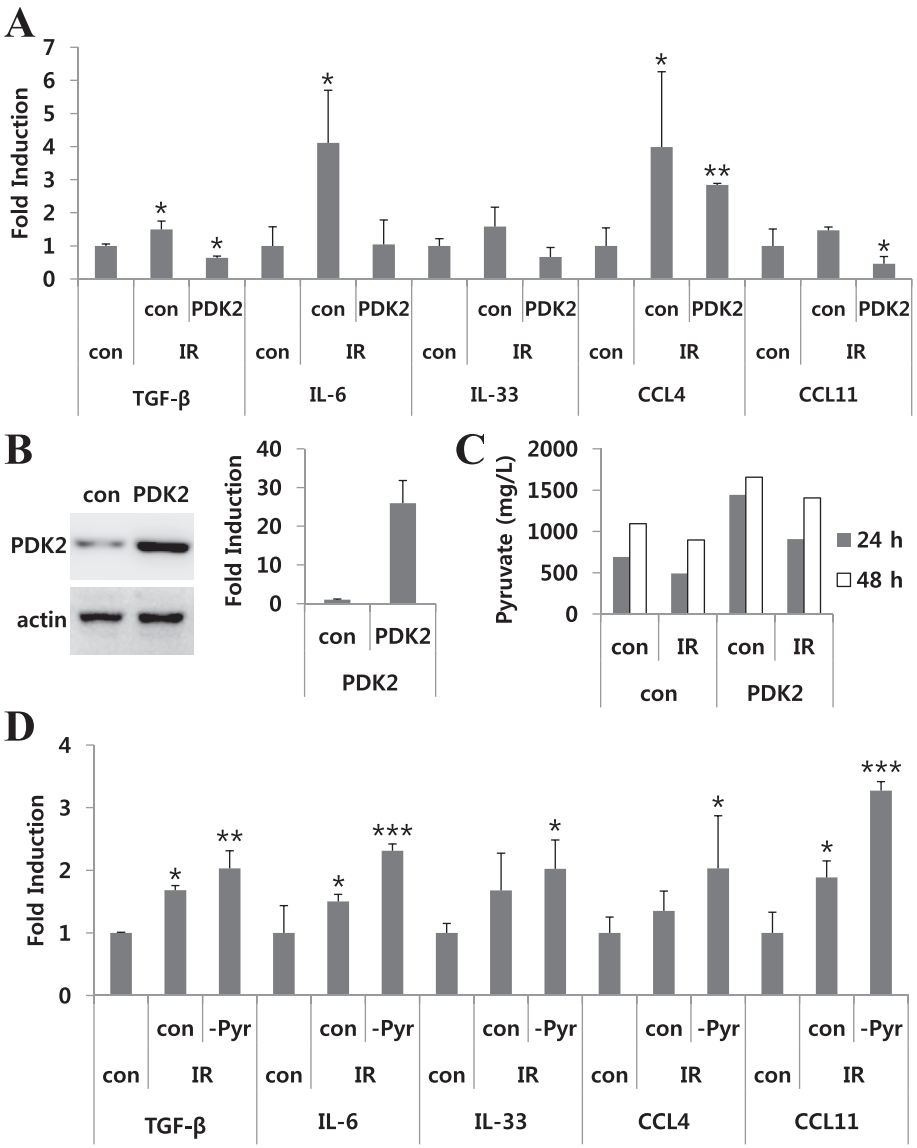

Fig. 3. Pyruvate dehydrogenase kinase 2 (PDK2) and pyruvate inhibited irradiation-mediated cytokine expression. PDK2-transfected and control NIH3T3 cells were irradiated (10 Gy) 24 h after transfection. A, B) Quantitative real-time PCR and western blotting showed that irradiation induced cytokine and chemokine gene expression. C) After irradiation, media were collected and assayed for pyruvate, as described in the Methods and Materials section. D) NIH3T3 cells were maintained for 24 h in pyruvate-free and normal media prior to irradiation. Cell lysates were then analyzed by quantitative real-time PCR, using the indicated primers. Error bars show standard deviation; *$p < 0.05$; **$p < 0.01$; ***$p < 0.001$. con: Normal DMEM media, −Pyr: pyruvate free DMEM media (methods and materials).

PDK family members are key regulators of pyruvate metabolism. Pyruvate is then converted either to acetyl-CoA (by PDC) for fatty acid synthesis during a fed state, or to oxaloacetate (by pyruvate carboxylase) for gluconeogenesis during a fasting state [6,7]. In this study, we investigated whether exogenous pyruvate reduced irradiation-induced inflammatory cytokine expression and mouse skin injury. A number of previous studies implicated a role for several pyruvate derivatives in the reduction of skin fibrosis, and pyruvate was shown to be a key regulator of several parameters related to the inflammatory response and tumorigenesis [24–26]. Further, pyruvate protected from ultraviolet B (UVB)-induced keratinocyte damage and dermal erythema [27,28]. Aromatic pyruvates (phenylpyruvate, 4-hydroxyphenylpyruvate, and indole-3-pyruvate) are also suggested to play an important role in protection from UVB-induced skin damage.

It has been reported that intraperitoneal injection of pyruvate (500–1000 mg/kg) in rats with transient forebrain ischemia almost completely prevented neuronal cell death [29]. In addition, Gupta et al. illustrated that sodium pyruvate (500 mg/kg) exhibited significant anti-inflammatory activity in models of inflammation; this could be attributed to its antioxidant properties [17]. Our studies also demonstrated that pyruvate treatment markedly downregulated the irradiation-induced increase in skin thickness. In our model, a 1-cm^2 collimator was used to administer a 50 Gy single dose to the dorsal skin of mouse. Although there is no perfect model for studying fibrosis, the dorsal skin radiation model offers a standardized method that has been used in our laboratory for many years [16]. To investigate the *in vivo* anti-skin fibrosis activity of pyruvate, mice were given an oral dose of pyruvate or vehicle control every two days after irradiation. Consistent with the *in vitro* data, we demonstrated that oral administration of pyruvate reduced irradiation-induced dermal hyperplasia and collagen fiber formation in mice.

The present study investigated the effect of pyruvate on irradiation-induced skin fibrosis and, more importantly, examined

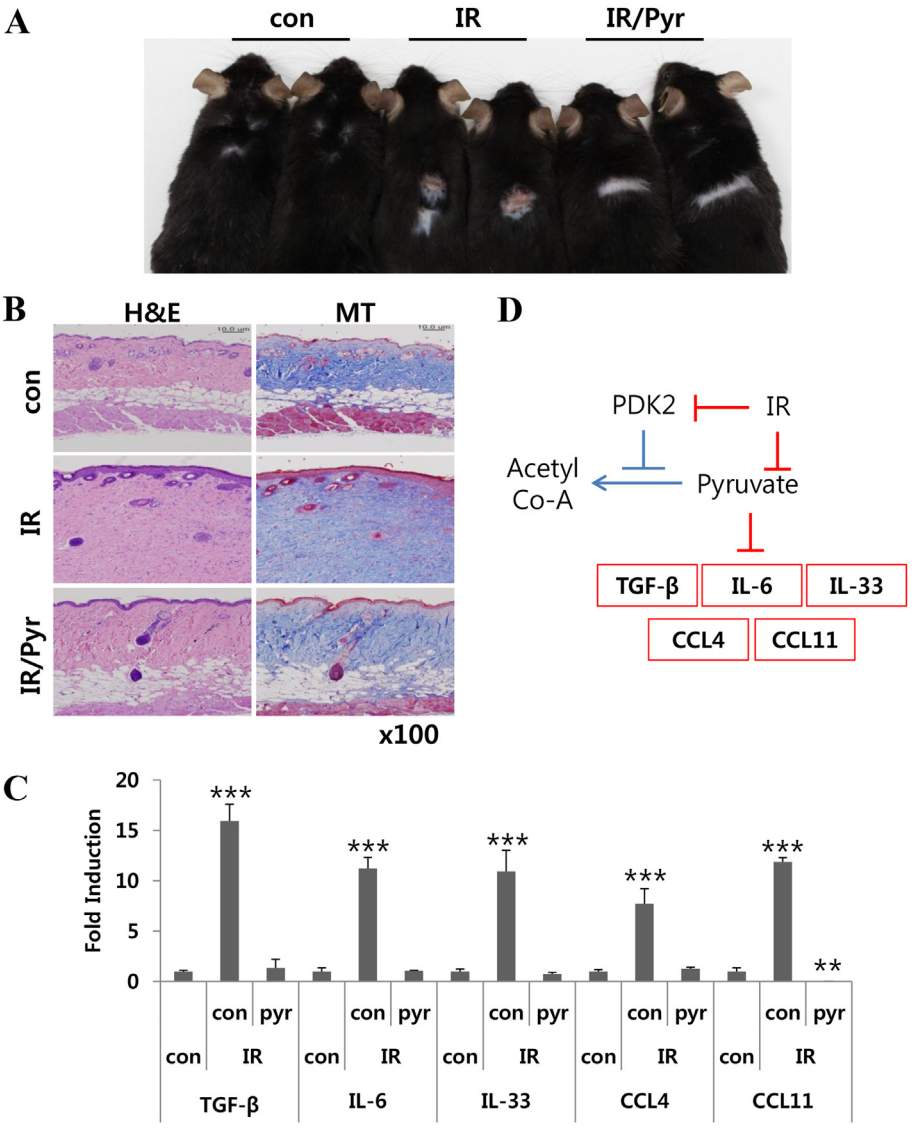

Fig. 4. Pyruvate inhibited the radiation-induced increase in skin thickness. A) We administrated 500 mg/kg oral pyruvate to C57BL/6 mice. Skin samples were obtained by punch biopsies after irradiation (50 Gy). B) Representative images of skin sections sampled at 6 weeks and stained with hematoxylin and eosin (H&E) or Masson's Trichrome (MT). Irradiated sections demonstrated marked thickening of both the epidermis and dermis. Immunohistochemical staining was performed on the mouse skin sections using the indicated antibody (×100). C) Cytokine and chemokine gene expression profiles in mouse skin, evaluated using quantitative real-time PCR. D) Schematic illustration of radiation-induced PDK2 inhibition. Error bars show standard deviation; **p < 0.01; ***p < 0.001). con: vehicle oral administration, Pyr: pyruvate oral administration.

the mechanisms underlying these effects. Taken together, our findings suggested that the therapeutic efficacy of pyruvate may be mediated by inhibition of PDK2 signaling, highlighting the potential use of pyruvate as a therapeutic agent for radiation-induced skin injury.

Funding

This work was supported by the Nuclear Research and Development Program (NRF-2011-0031695) and by the Radiation Technology Research and Development Program (NRF-2013M2A2A7042978) through the National Research Foundation of Korea, funded by the Ministry of Science, ICT & Future Planning as well as by a faculty research grant from Yonsei University College of Medicine for 2014 (6-2014-0031).

Conflict of interest

There are no conflicts of interest to declare.

Appendix A. Supplementary data

Supplementary data related to this article can be found at http://dx.doi.org/10.1016/j.bbrc.2015.03.060.

Transparency document

Transparency document related to this article can be found online at http://dx.doi.org/10.1016/j.bbrc.2015.03.060.

References

[1] J.H. Kim, A.J. Kolozsvary, K.A. Jenrow, S.L. Brown, Mechanisms of radiation-induced skin injury and implications for future clinical trials, Int. J. Radiat. Biol. 89 (2013) 311–318.
[2] J.L. Ryan, Ionizing radiation: the good, the bad, and the ugly, J. Invest. Dermatol. 132 (2012) 985–993.
[3] C. Nieder, F.B. Zimmermann, M. Adam, M. Molls, The role of pentoxifylline as a modifier of radiation therapy, Cancer Treat. Rev. 31 (2005) 448–455.
[4] J.L. Lefaix, S. Delanian, M.C. Vozenin, J.J. Leplat, Y. Tricaud, M. Martin, Striking regression of subcutaneous fibrosis induced by high doses of gamma rays

using a combination of pentoxifylline and alpha-tocopherol: an experimental study, Int. J. Radiat. Oncol. Biol. Phys. 43 (1999) 839–847.
[5] R.J. DeBerardinis, A. Mancuso, E. Daikhin, I. Nissim, M. Yudkoff, S. Wehrli, C.B. Thompson, Beyond aerobic glycolysis: transformed cells can engage in glutamine metabolism that exceeds the requirement for protein and nucleotide synthesis, Proc. Natl. Acad. Sci. U. S. A. 104 (2007) 19345–19350.
[6] M.C. Sugden, M.J. Holness, Mechanisms underlying regulation of the expression and activities of the mammalian pyruvate dehydrogenase kinases, Arch. Physiol. Biochem. 112 (2006) 139–149.
[7] M.S. Patel, L.G. Korotchkina, Regulation of mammalian pyruvate dehydrogenase complex by phosphorylation: complexity of multiple phosphorylation sites and kinases, Exp. Mol. Med. 33 (2001) 191–197.
[8] M.M. Bowker-Kinley, W.I. Davis, P. Wu, R.A. Harris, K.M. Popov, Evidence for existence of tissue-specific regulation of the mammalian pyruvate dehydrogenase complex, Biochem. J. 329 (Pt 1) (1998) 191–196.
[9] A.M. Bolger, M. Lohse, B. Usadel, Trimmomatic: a flexible trimmer for illumina sequence data, Bioinformatics 30 (2014) 2114–2120.
[10] C. Trapnell, L. Pachter, S.L. Salzberg, TopHat: discovering splice junctions with RNA-Seq, Bioinformatics 25 (2009) 1105–1111.
[11] H. Li, B. Handsaker, A. Wysoker, T. Fennell, J. Ruan, N. Homer, G. Marth, G. Abecasis, R. Durbin, S. Genome project data processing, the sequence alignment/map format and SAMtools, Bioinformatics 25 (2009) 2078–2079.
[12] S. Anders, HTSeq: Analysing High-throughput Sequencing Data with Python, 2010. http://www-huber.embl.de/users/anders/HTSeq/doc/overview.html.
[13] S. Anders, Analysing RNA-Seq data with the DESeq package, Mol. Biol. (2010) 1–17.
[14] W. Huang da, B.T. Sherman, R.A. Lempicki, Systematic and integrative analysis of large gene lists using DAVID bioinformatics resources, Nat. Protoc. 4 (2009) 44–57.
[15] C.M. Ma, C.W. Coffey, L.A. DeWerd, C. Liu, R. Nath, S.M. Seltzer, J.P. Seuntjens, M. American Association of Physicists, AAPM protocol for 40–300 kV X-ray beam dosimetry in radiotherapy and radiobiology, Med. Phys. 28 (2001) 868–893.
[16] V.D. Thanik, C.C. Chang, R.A. Zoumalan, O.Z. Lerman, R.J. Allen Jr., P.D. Nguyen, S.M. Warren, S.R. Coleman, A. Hazen, A novel mouse model of cutaneous radiation injury, Plastic Reconstr. Surg. 127 (2011) 560–568.
[17] S.K. Gupta, S. Rastogi, J. Prakash, S. Joshi, Y.K. Gupta, L. Awor, S.D. Verma, Anti-inflammatory activity of sodium pyruvate—a physiological antioxidant, Indian J. Physiol. Pharmacol. 44 (2000) 101–104.
[18] G.N. Neigh, S.D. Bilbo, A.K. Hotchkiss, R.J. Nelson, Exogenous pyruvate prevents stress-evoked suppression of mitogen-stimulated proliferation, Brain Behav. Immun. 18 (2004) 425–433.
[19] K.H. Sit, Y.K. Lau, S.E. Aw, Differential oxygen sensitivities in G6PDH activities of cultured keloid and normal skin dermis single cells, J. Dermatol. 18 (1991) 572–579.
[20] N. Yevdokimova, S. Podpryatov, The up-regulation of angiotensin II receptor type 1 and connective tissue growth factor are involved in high-glucose-induced fibronectin production by cultured human dermal fibroblasts, J. Dermatol. Sci. 47 (2007) 127–139.
[21] A.S. Vincent, T.T. Phan, A. Mukhopadhyay, H.Y. Lim, B. Halliwell, K.P. Wong, Human skin keloid fibroblasts display bioenergetics of cancer cells, J. Invest. Dermatol. 128 (2008) 702–709.
[22] F. Zwicker, A. Kirsner, P. Peschke, F. Roeder, J. Debus, P.E. Huber, K.J. Weber, Dichloroacetate induces tumor-specific radiosensitivity in vitro but attenuates radiation-induced tumor growth delay in vivo, Strahlenther. Onkol. Organ Dtsch. Rontgengesellschaft. 189 (2013) 684–692.
[23] W. Saleem, Y. Suzuki, A. Mobaraki, Y. Yoshida, S. Noda, J.I. Saitoh, T. Nakano, Reduction of nitric oxide level enhances the radiosensitivity of hypoxic non-small cell lung cancer, Cancer Sci. 102 (2011) 2150–2156.
[24] M.P. Fink, Ethyl pyruvate: a novel anti-inflammatory agent, J. Intern. Med. 261 (2007) 349–362.
[25] K.K. Kao, M.P. Fink, The biochemical basis for the anti-inflammatory and cytoprotective actions of ethyl pyruvate and related compounds, Biochem. Pharmacol. 80 (2010) 151–159.
[26] Y. Takakusagi, S. Matsumoto, K. Saito, M. Matsuo, S. Kishimoto, J.W. Wojtkowiak, W. DeGraff, A.H. Kesarwala, R. Choudhuri, N. Devasahayam, S. Subramanian, J.P. Munasinghe, R.J. Gillies, J.B. Mitchell, C.P. Hart, M.C. Krishna, Pyruvate induces transient tumor hypoxia by enhancing mitochondrial oxygen consumption and potentiates the anti-tumor effect of a hypoxia-activated prodrug TH-302, PloS One 9 (2014) e107995.
[27] R. Aoki, A. Aoki-Yoshida, C. Suzuki, Y. Takayama, Protective effect of indole-3-pyruvate against ultraviolet b-induced damage to cultured HaCaT keratinocytes and the skin of hairless mice, PloS One 9 (2014) e96804.
[28] A. Aoki-Yoshida, R. Aoki, Y. Takayama, Protective effect of pyruvate against UVB-induced damage in HaCaT human keratinocytes, J. Biosci. Bioeng. 115 (2013) 442–448.
[29] J.Y. Lee, Y.H. Kim, J.Y. Koh, Protection by pyruvate against transient forebrain ischemia in rats, J. Neurosci. Off. J. Soc. Neurosci. 21 (2001) RC171.